

Parameters and States Estimation by Moving Horizon Estimation, High Gain Observer and Unscented Kalman Filter of a Doubly-Fed Induction Generator Driven by Wind Turbine: A Comparative Study

Steve Alan TALLA OUAMBO¹, Alexandre Teplaira BOUM^{2,*} and Adolphe MOUKENGUE IMANO¹

¹Department of Physics, Faculty of Science, the University of Douala, Cameroon, 24157 Douala, Cameroon

²University of Douala, ENSET, 1872 Douala, Cameroon

Received 2 December 2017; Accepted 30 March 2018

Abstract

This paper presents a general framework for the doubly fed induction generator (DFIG), apply and analyze the behavior of three estimation techniques, which are the Unscented Kalman Filter (UKF), the High Gain Observer (HGO) and the Moving Horizon Estimation (MHE), for parameters estimation of the doubly fed induction generator (DFIG) driven by wind turbine. A comparison of those techniques has been made under different aspects notably, computation time and estimation accuracy in two modes of operation of the DFIG, the healthy mode and the faulty mode. The performance of the MHE has been clearly superior to other estimators during our experiments.

Keywords: Doubly-Fed Induction Generator, High Gain Observer, Unscented Kalman Filter, Moving Horizon Estimation, parameters estimation

1. Introduction

Nowadays most of generated electricity comes from non-renewable sources of fuel. These products transfer to the atmosphere an important quantities of CO₂, and inescapably leading to the warming up of the atmosphere [1]. The production of the wind energy spreads through the world, and significantly, it imposed itself during the past decade [2]. Doubly-fed induction generators (DFIGs) are actually the most used wind power generators in many countries [3]. Therefore, many contributions have been made to the inverters and converters usually in DFIG used in the power electronics domain [4]. A doubly fed induction generator model for transient stability analysis has been proposed in [5], in which authors focused their study on the control loops of instantaneous response. In [6], authors have been proposed some robust observers to estimate states and actuator faults for different class of linear and nonlinear systems at the same instant. Though systems are becoming more and more complex, DFIG can be subject by many types of faults [7], diagnosis and faults estimation issues have become primordial to ensure a good supervision of systems and guarantee the safety of materials and operators (humans) [8]. A survey based on current sensor fault detection and isolation and control reconfiguration current for doubly fed induction generator has been proposed by [9]. Studies led by [10], have contributed to an adaptive parameter estimation algorithm used for estimating the rotor resistance of the DFIG, however, the others parameters were assumed to be constant. To improve the Extended Kalman Filter (EKF), a new nonlinear filtering algorithm named the Unscented Kalman Filter (UKF) has been developed in [11]. Widely used in some fields, UKF has been found in several

studies such as training of neural networks [12], multi-sensor fusion for instance. This paper investigate the usage of the Unscented Kalman Filter UKF, High Gain Observer (HGO) and the Moving Horizon Estimator (MHE) to estimate the dynamic states and electrical parameters of the wind turbine system. These estimates can be used to enhance the performance of Doubly Fed Induction Generator in power systems, for rotor and stator resistances faults in the circumstances where internal states will be involved in a control design [3] and the acquisition of internal states, which are relatively difficult to get can realized from the dynamic state estimation and for monitoring purposes. The paper is organized as follows: in section II, the mathematical model for DFIG is presented, followed by the description of estimation algorithms in section III. The results of the parameter estimation tests are presented in section IV. Finally section V gives the conclusions.

2. Mathematical Model for DFIG

In this section, we deal with the mathematical modeling of the DFIG-based wind energy system, we will only describe the wind turbine (also called drive train), and the asynchronous generator (also called induction generator) because this paper focuses on estimating of the parameters and dynamic states of the DFIG Figure 1.

Two frames of reference are used in this model: stator voltage ($d - q$) reference frame, and mutual flux ($d - q$) reference frame. And in Table 4 and Table 5, all parameters and constants are given.

2.1. Modeling of the wind turbine

From the wind, the power extracted can give the mechanical torque. The energy from the wind is extracted from the wind turbine and converted into mechanical power [14]. The wind

*E-mail address: boumat2002@yahoo.fr

turbine model is based on the output power characteristics, as Equations (1) and (2), [15].

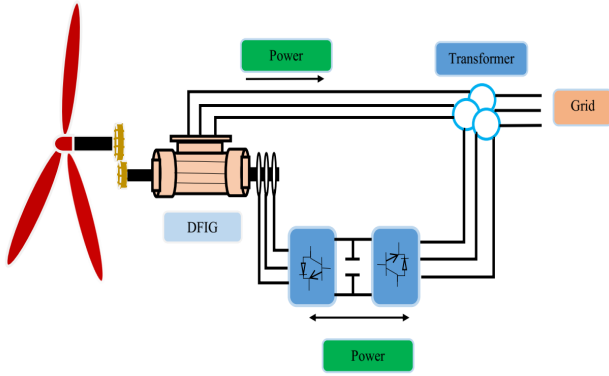


Fig. 1. Configuration of DFIG-based wind turbine system [13]

$$P_m = C_p(\lambda, \beta) \frac{1}{2} \rho A v_w^3 = C_p(\lambda, \beta) E_w \quad (1)$$

$$\lambda_{TS} = \frac{R\omega_t}{v_w} \quad (2)$$

Where the aerodynamic extracted power is P_m , which depends on C_p , the efficiency coefficient. The air density ρ , the turbine swept area A , and the wind speed v_w . The kinetic energy contained in the wind at a particular wind speed is given by E_w . The blade radius and angular frequency of rotational turbine are R and ω_t respectively. $C_p(\lambda; \beta)$ the efficiency coefficient depends on tip speed ratio λ_{TS} and blade pitch angle β , determines the amount of wind kinetic energy that can be captured by the wind turbine system [13]. $C_p(\lambda; \beta)$ can be describe as:

$$C_p(\lambda, \beta) = 0.5 \left(\frac{116}{\lambda_i} - 0.4\beta - 5 \right) e^{-21/\lambda_i} \quad (3)$$

Where

$$\frac{1}{\lambda_i} = \frac{1}{\lambda_{TS} + 0.08\beta} - \frac{0.035}{\beta^3 + 1} \quad (4)$$

2.2. Modeling of the Asynchronous Generator

For the induction generator, the Park model is the model that is commonly used [16]. After applying the synchronously rotating reference frame transformation to the stator and rotor fluxes equations of the generator, the following differential equations describe the dynamics of the rotor and stator fluxes [17]:

$$\begin{cases} \dot{\Phi}_{dr} = w_b(v_{dr} + (w_s - w_r)\Phi_{qr} - R_r i_{dr}) \\ \dot{\Phi}_{qr} = w_b(v_{qr} - (w_s - w_r)\Phi_{dr} - R_r i_{qr}) \\ \dot{\Phi}_{ds} = w_b(v_{ds} + w_s\Phi_{qs} - R_s i_{ds}) \\ \dot{\Phi}_{qs} = w_b(v_{qs} - w_s\Phi_{ds} - R_s i_{qs}) \end{cases} \quad (5)$$

Where $w_s = 1$ is the synchronous angular speed in the synchronous frame and $w_b = 2\pi f$ rad/s is the base angular speed, with $f = 60$ Hz. With additional variables stator-rotor

mutual flux Φ_{dm} and Φ_{qm} , rotor current i_{dr} and i_{qr} and stator current i_{ds} and i_{qs} can be expressed as:

$$\begin{cases} i_{dr} = \frac{\Phi_{dr} - \Phi_{dm}}{L_{lr}} \\ i_{qr} = \frac{\Phi_{qr} - \Phi_{qm}}{L_{lr}} \end{cases} \quad (6)$$

$$\begin{cases} i_{ds} = \frac{\Phi_{ds} - \Phi_{dm}}{L_{ls}} \\ i_{qs} = \frac{\Phi_{qs} - \Phi_{qm}}{L_{ls}} \end{cases} \quad (7)$$

Where

$$\Phi_{dm} = L_{ad} \left(\frac{\Phi_{dr}}{L_{lr}} + \frac{\Phi_{ds}}{L_{ls}} \right) \quad (8)$$

$$\Phi_{qm} = L_{aq} \left(\frac{\Phi_{qr}}{L_{lr}} + \frac{\Phi_{qs}}{L_{ls}} \right)$$

are the stator-rotor mutual flux.

Where constants L_{ad} and L_{aq} are the (d - q) mutual flux factors, expressed as:

$$L_{ad} = L_{aq} = \frac{1}{\frac{1}{L_m} + \frac{1}{L_{ls}} + \frac{1}{L_{lr}}} \quad (9)$$

The relationship between mechanical torque T_m , electrical torque T_e and rotor speed w_r , can be shown by the following differential equation,

$$\dot{w}_r = \frac{1}{2H} (T_m - T_e - F w_r) \quad (10)$$

Where constant F is the friction factor and H is the generator inertia, and T_e , the electrical torque which can be expressed as:

$$T_e = \Phi_{ds} i_{qs} - \Phi_{qs} i_{ds} \quad (11)$$

These equations are derived in [4] and all parameters are defined in per unit based on the generator ratings and synchronous speed.

3. Estimation algorithms

3.1. High Gain Observer[18]

This observer class is applied for nonlinear system classes of the form (12). Its applications are so large [19]. We briefly present the developed survey in [20] that points up the synthesis of observers adapted to the observable nonlinear systems. Consider the following nonlinear system:

$$\begin{cases} \dot{x} = f(x) + g(x)u \\ y = h(x) \end{cases} \quad (12)$$

Where $x \in R^n, u \in R^m, y \in R^s$

First, the system (12) must be uniformly locally observable, and then it will be possible to make the variable change $z = T(x)$ that will transform the system (12) in the following form:

$$\begin{cases} \dot{z} = Az + \varphi(u, z) \\ y = Cz \end{cases} \quad (13)$$

The observer must satisfy the following theorem [20]:

- i. The function φ is globally Lipschitz uniformly to

$$\text{Let } K = \begin{bmatrix} K_1 & & \\ & \ddots & \\ & & K_p \end{bmatrix} \text{ an adequate size matrix such as,}$$

for every K_j block, the matrix

$A_k - K_k C_k$ should give all its eigenvalues with negative real part:

Let's suppose that there exists two integer sets $\{\sigma_1, \dots, \sigma_n \in Z\}$ and $\{\delta_1 > 0, \dots, \delta_p > 0 \in N^*\}$ such as:

- ii. $\sigma_{\mu_k+v} = \sigma_{\mu_k+v-1} + \delta_p, k = 1, \dots, p, v = 1, \dots, \eta_k - 1$
iii. $\frac{\partial \varphi_i}{\partial z_j} \neq 0 \Rightarrow \sigma_i \geq \sigma_j, i, j = 1, \dots, n, j \neq \mu_k, k = 1, \dots, p$

So,

$$\dot{\hat{z}} = A\hat{z} + \varphi(\hat{z}, u) - S_\theta^{-1}K(C\hat{z} - y) \quad (14)$$

is an exponential observer for the system (13) as well.

And there exists T_l such as, for all $T, 0 < T < T_l$.

With,

$$S(S, \delta) = \begin{bmatrix} S^{\delta_1} \Delta(S^{\delta_1}) & & \\ & \ddots & \\ & & S^{\delta_p} \Delta(S^{\delta_p}) \end{bmatrix}$$

$$\Delta_\theta(S) = \begin{bmatrix} 1 & & & \\ & S & & \\ & & \ddots & \\ & & & S^{\eta_\theta-1} \end{bmatrix}$$

By operating a reverse variable change for coming back to the initial nonlinear system, the observer for the system (12) is given by:

$$\dot{\hat{x}} = f(\hat{x}) + g(\hat{x})u - \left(\frac{\partial \Gamma}{\partial \hat{x}}(\hat{x}(t)) \right)^{-1} S_\theta^{-1}(h(\hat{x}) - y) \quad (15)$$

\hat{x} : Estimated value of x .

Γ : An application $R^n \rightarrow R^n$.

With,

$$\Gamma = [h_1, L_f h_1, L_f^2 h_1, \dots, L_f^{\delta_1} h_1, h_2, L_f h_2, L_f^2 h_2, \dots, L_f^{\delta_2} h_2, \dots, h_p, L_f h_p, L_f^2 h_p, \dots, L_f^{\delta_p} h_p]^T$$

And $L_f^{\delta_k}$ is the Lie δ_k^i derivative.

P : Number of outputs.

And S_θ satisfies the following Lyapunov relation:

$$\dot{S} = -\theta S_\theta - A^T S_\theta - S_\theta A + C^T C = 0 \quad (16)$$

In [20], the demonstration is done.

3.2. The Unscented Kalman Filter

The Unscented Kalman Filter (UKF) has been essentially designed for the state estimation problems, and applied in some nonlinear control applications [11]. The Unscented Kalman Filter (UKF) compensates for approximation issues of the Extended Kalman Filter (EKF). A Gaussian random variable represents the state distribution, which is specified using a set of sample points chosen very carefully [12]. The unscented transformation (UT) is a method to estimate or calculate statistics of a random variable which is subjected to a nonlinear transformation [11]. In stochastic estimation problems, a common assumption usually is used which underline the fact that the process and measurement noise terms are additive, as in:

$$\begin{aligned} x_k &= f(x_{k-1}, u_{k-1}) + w_{k-1} \\ y_k &= h(x_k, u_k) + v_k \end{aligned} \quad (17)$$

The dimension of the sigma-points is the same as the state vector, that is to say $L = n_x$. The UKF is recursively executed, starting with the assumed initial conditions \hat{x}_0 and P_0 . First a set of sigma-points are generated from the prior state estimate \hat{x}_{k-1} and covariance P_{k-1} at each discrete-time step, as in:

$$\chi_{k-1} = \left[\hat{x}_{k-1} \quad \hat{x}_{k-1} + \sqrt{L + \lambda} \sqrt{P_{k-1}} \quad \hat{x}_{k-1} - \sqrt{L + \lambda} \sqrt{P_{k-1}} \right] \quad (18)$$

For the next point, each sigma point is passed through the state prediction function f that is nonlinear.

$$\chi_{k,k-1}^{(i)} = f(\chi_{k-1}^{(i)}, u_{k-1}), \quad i = 0, 1, 2, \dots, 2L \quad (19)$$

$\chi_{k,k-1}$ means that this is the predicted value of the sigma-point based on the information from the prior time step. Sigma-points transformed, the post transformation mean and covariance are computed using weighted averages of the transformed sigma-points [21],

$$\hat{x}_{k,k-1} = \sum_{i=0}^{2L} \eta_i^m \chi_{k,k-1}^{(i)} \quad (20)$$

$$P_{k,k-1} = Q_{k-1} + \sum_{i=0}^{2L} \eta_i^c (\chi_{k,k-1}^{(i)} - \hat{x}_{k,k-1})(\chi_{k,k-1}^{(i)} - \hat{x}_{k,k-1})^T \quad (21)$$

where $\eta_0^m = \lambda / (L + \lambda)$ and $\eta_0^c = \lambda / (L + \lambda) + 1 - \alpha^2 + \beta$. The measurement noise is also omitted from the observation function, as for the prediction as in:

$$\psi_{k,k-1}^{(i)} = h(\chi_{k,k-1}^{(i)}, u_k) \quad (22)$$

Where is a matrix of output sigma-points. Output sigma-points are used to calculate output covariance matrix, the predicted output and cross-covariance by using:

$$\begin{aligned} \hat{y}_{k,k-1} &= \sum_{i=0}^{2L} \eta_i^m \psi_{k,k-1}^{(i)} \\ P_k^{yy} &= R_k + \sum_{i=0}^{2L} \eta_i^c (\psi_{k,k-1}^{(i)} - \hat{y}_{k,k-1}) (\psi_{k,k-1}^{(i)} - \hat{y}_{k,k-1})^T \\ P_k^{xy} &= \sum_{i=0}^{2L} \eta_i^c (\chi_{k,k-1}^{(i)} - \hat{x}_{k,k-1}) (\psi_{k,k-1}^{(i)} - \hat{y}_{k,k-1})^T \end{aligned} \quad (23)$$

Due to the additive noise assumption, R is added to the output covariance matrix. For calculating the Kalman gain matrix K , covariance matrices are used, using:

$$K_k = P_k^{xy} (P_k^{yy})^{-1} \quad (24)$$

And then this Kalman gain matrix is used to update covariance estimates and the state, as in:

$$\begin{aligned} \hat{x}_k &= \hat{x}_{k,k-1} + K_k (y_k - \hat{y}_{k,k-1}) \\ P_k &= P_{k,k-1} - K_k P_k^{yy} K_k^T \end{aligned} \quad (25)$$

With y_k , the measurement vector, \hat{x}_k is the a posteriori state and P_k is the covariance estimates

3.3. The Moving Horizon Estimation[22]

The moving horizon estimation is a powerful means of estimating the states, and having in particular the possibility to constrain the outputs, states and noises. We can be described it as a least-squares optimization that leads to a states' estimation and working with a limited amount of information. Its particularity is to avoid the recursive manner characteristic of the extended Kalman filter. Under different approaches, several researchers [23,24,25,26] studied it, however presenting many similarities. The moving and full state estimations almost follow the same steps. In the moving state estimation, variables can be handled contrary to the full state estimation. In the full state estimation, at current time k , all variables from initial time $n = 0$ to $n = k$ are used in the calculation. With a horizon H , the moving state estimation uses in the calculation only the concerned variables (, measured outputs, manipulated inputs and estimated states) from $n = k + 1 - H$ to $n = k$, a moving vectors collect them. First of all, consider the full state estimation problem. Let assume that the process can be represented by the following continuous-time model:

$$\dot{x}(t) = f(x(t), u(t)) + Gw(t) \quad (26)$$

Where w_k is the control noise.

Where the Gaussian noise of zero mean is w . We can describe the measured outputs y by the discrete-time model

$$y_k = h(x_k) + v_k \quad (27)$$

Where v_k is the observation noise.

The equivalent linear discrete model is given by:

$$x_{k+1} = Ax_k + Bu_k + Gw_k \quad (28)$$

Where the matrices A and B are the Jacobian matrices with respect to f in relation to x_k and u_k respectively. The measurement model is linearized as:

$$y_{k+1} = Cx_{k+1} + v_{k+1} \quad (29)$$

Where the matrix C is the Jacobian matrix of h with respect to x_k . In the full state estimation problem, we have to minimize the following criterion with respect to the sequence of noises $\{w_0, \dots, w_{k-1}\}$ and to the initial state x_0 , and then the states \hat{x}_i are obtained by using equation (28).

$$J_k = (x_0 - \hat{x}_0)^T \Pi_0^{-1} (x_0 - \hat{x}_0) + \sum_{i=0}^{k-1} (v_{i+1}^T R^{-1} v_{i+1} + w_i^T Q^{-1} w_i) \quad (30)$$

The weighting matrices Π_0^{-1} , Q^{-1} and R^{-1} respectively symbolize the initial estimation, the confidence in the dynamic model and the measurements. The main disadvantage of full state estimation is that during the computation we notice the size of the optimization problem grows as time increases, and would likely cause a failure in the optimization. The favorable solution to this increasing size is to set the problem according to a moving-horizon approach.

Let us consider the problem of moving state estimation. The criterion (30) is split into two parts [24, 25]:

$$J_k = J_{k-H} + \sum_{i=k-H}^{k-1} (v_{i+1}^T R^{-1} v_{i+1} + w_i^T Q^{-1} w_i) = J_{k-H} + J^{mhe} \quad (31)$$

The second term J^{mhe} of the criterion (31) depends on the sequence of noises $\{w_{k-H}, \dots, w_{k-1}\}$ and on the state x_{k-H} .

Assume that $k > H$ and set the optimized criterion:

$$J_{k-H}^* = \min_{x_0, w_0, \dots, w_{k-H-1}} J_{k-H} \quad (32)$$

And then, in the full optimized criterion becomes:

$$J_k^* = \min_{x_0, w_0, \dots, w_{k-1}} J_k \quad (33)$$

$$= \min_{z, w_{k-H}, \dots, w_{k-1}} \left[\sum_{i=k-H}^{k-1} (v_{i+1}^T R^{-1} v_{i+1} + w_i^T Q^{-1} w_i) \right] + J_{k-H}^*(z) \quad (34)$$

Where z is the arrival state x_{k-H} based on the optimized variables $\{w_{k-H}^*, \dots, w_{k-H-1}^*\}$ and x_0 .

In practice, it is very complicated and almost impossible to really minimize $J_{k-H}(z)$ when k becomes large enough as this would be a full estimation problem again. The recommend solution is to retain the previous values of the

optimized criterion J_k^* obtained by moving horizon estimation denoted by $J_k^{mhe}(z)$ along time k and to approximate $J_{k-H}(z)$ as :

$$J_{k-H}(z) \approx (z - \hat{x}_{k-H}^{mhe})^T \Pi_{k-H}^{-1} (z - \hat{x}_{k-H}^{mhe}) + J_{k-H}^{mhe}(z) \quad (35)$$

Where \hat{x}_{k-H}^{mhe} is the state estimated by moving horizon observer at time $(k - H)$. Under these assumptions, the criterion (31) becomes:

$$J_k = \sum_{i=k-H}^{k-1} (v_{i+1}^T R^{-1} v_{i+1} + w_i^T Q^{-1} w_i) + (z - \hat{x}_{k-H}^{mhe})^T \Pi_{k-H}^{-1} (z - \hat{x}_{k-H}^{mhe}) + J_{k-H}^{mhe}(z) \quad (36)$$

The discrete Riccati equation we used for the covariance matrix of the Kalman filter is called to update Π_k :

$$\Pi_k = A \Pi_{k-1} A^T + G Q G^T - A \Pi_{k-1} C^T [C \Pi_{k-1} C^T + R]^{-1} C \Pi_{k-1} A^T \quad (37)$$

With Π_0 given. The Moving horizon estimation algorithm is described by the diagram in Figure (2)

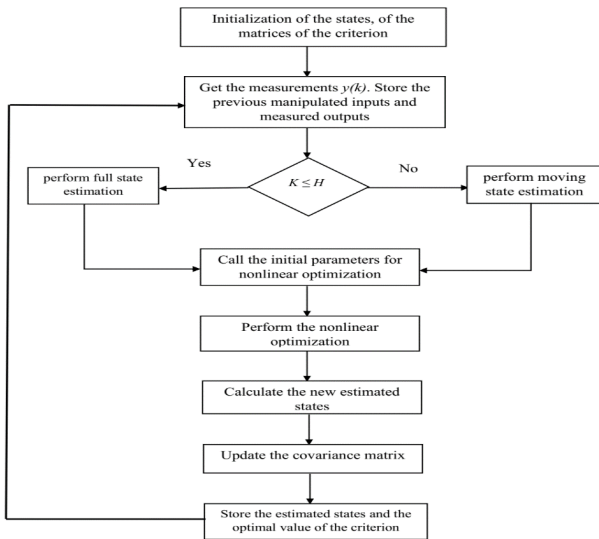


Fig. 2. MHE algorithm

4. Numerical results

In this section, the performances of the proposed observers are illustrated in simulation. Observers' algorithms have been implemented in MATLAB/SIMULINK software. The Doubly-Fed Induction Generator system states which have been used for estimation are expressed into a vector x , this vector includes as parameters to estimate the stator and rotor resistances, as follows:

$$x = \left[\Phi_{ds} \quad \Phi_{qs} \quad \Phi_{dr} \quad \Phi_{qr} \quad R_s \quad R_r \right]^T \quad (38)$$

The inputs of the system are the rotor angular electrical speed, stator and rotor voltages, as in:

$$u = \left[v_{ds} \quad v_{qs} \quad v_{dr} \quad v_{qr} \quad \omega_r \right]^T \quad (39)$$

The d and q axis of stator and rotor currents and the mechanical torque constitute the measurements of the systems,

$$y = \left[T_m \quad i_{ds} \quad i_{qs} \quad i_{dr} \quad i_{qr} \right]^T \quad (40)$$

Table 8 shows a comparison of the running time of High Gain Observer (HGO), the Unscented Kalman Filter (UKF), and the Moving Horizon Estimation (MHE) for the DFIG system. The High Gain observer being the fastest among the three methods under various modes especially the healthy mode which represents a healthy DFIG and the faulty mode where stator and rotor resistance would have changed value during the operation of the DFIG. Tables 7 and 6 gives the parameters of UKF and MHE only. For the UKF, the primary, secondary, and tertiary scaling parameters α , β and κ are chosen as 1, 2, and 0 respectively.

Figure 3 shows the generated estimates of the rotor and stator resistances by the HGO, UKF and the MHE in the healthy mode of working of the DFIG. Nevertheless, Figure 4 shows the generated estimates of the rotor and stator resistances by the HGO, UKF and the MHE in the faulty mode of working, let us mention that faulty mode is simply a mode where the DFIG undergoes a fault on its stator and/or rotor resistances during the operation. We just simulated those scenarios to appreciate the estimation performance of different observers in particular the HGO, UKF and MHE for process monitoring or diagnostics purposes. We can observe that the estimates by the MHE converges to the actual parameters in fewer time compared to the HGO and UKF. In Table 8, we notice the total computation time to obtain an estimate for the HGO algorithm is about 1.200 seconds, for the UKF algorithm is also about 1.190 seconds while the MHE algorithm took 152.978 seconds to estimate the parameters in the normal mode of working, and in the faulty mode, we have about 1.901 seconds, 1.666 seconds and 154.234 seconds for those observers respectively. We can conclude that when the asynchronous machine has a stator or rotor resistance fault, the estimation time increases. The reason the MHE algorithm takes longer to make an estimate is that in simulation, the optimization of the objective function, through a nonlinear programming algorithm has been performed at each time step, in this case study the nonlinear programming algorithm used is the sequential quadratic programming in the MATLAB in-built function *fmincon*. For the HGO we can underline this, a big value of θ leads to consolidate the linear part and to guarantee the stability of the nonlinear part through the fact that φ is imposed globally Lipschitz in relation to x [27]. If θ are big enough, the time of convergence decreases, but the observation becomes extremely sensitive to the measurement noises. A small value of θ leads to the reverse effect obviously. In comparison with the extended Kalman filter, this observer contains a lot less of setting variables that facilitates its optimization. Besides the number of equations to solve are a lot weaker and it decreases the time of calculation considerably. To know that the number of differential equations to solve for the Kalman filter is of

$n + \frac{n(n+1)}{2}$ such as n is the size of observation vector, when that number is n for the High gain observer [18], for our experiment the value of the gain is $\theta = 27$, on the other hand, the UKF algorithm has to handle $2L + 1$ sigma points and associated weights to represent state of the system. Tables 1 and 2 show the standard deviation and the variance of the estimation error. The comparison of these observers can be made by finding the mean squared error (MSE) value. The MSE can be evaluated as:

$$MSE = \frac{1}{N \times n} \sum_{i=1}^N (\theta_i - \hat{\theta}_i)^2 \quad (41)$$

Where N is the number of time steps, n is the dimension of state vector, θ_i is the simulated value and $\hat{\theta}_i$ is the estimated value from the filters. Table 3 shows a comparison of the three observers by finding the mean squared error in the healthy and the faulty mode of operation of the DFIG and we can notice that generally, the mean squared error of states and parameters in faulty mode is relatively greater than those in the healthy mode because of the fault occurring suddenly during the operation, but we can always see the high performance of the Moving Horizon Estimation on the others observers.

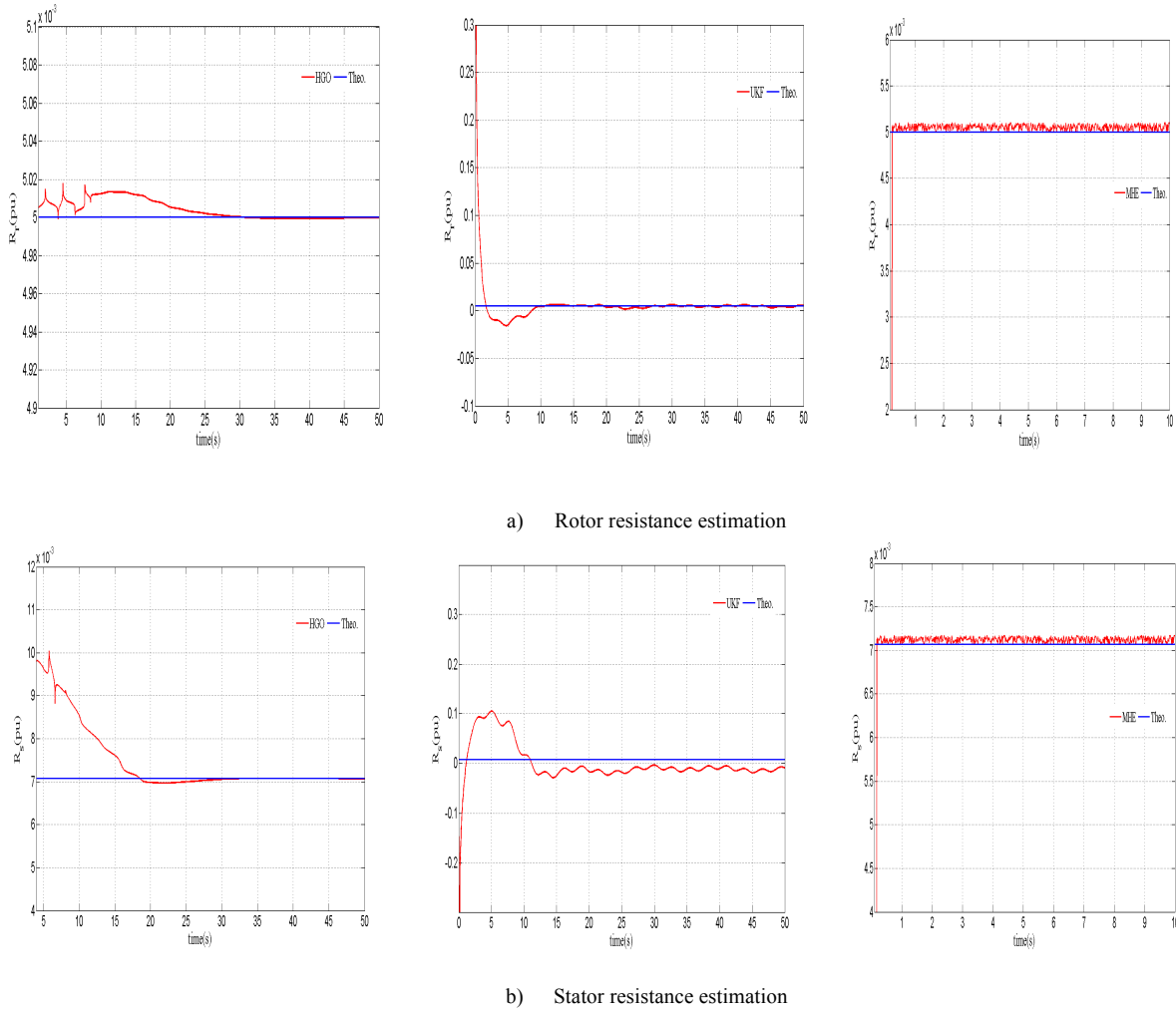


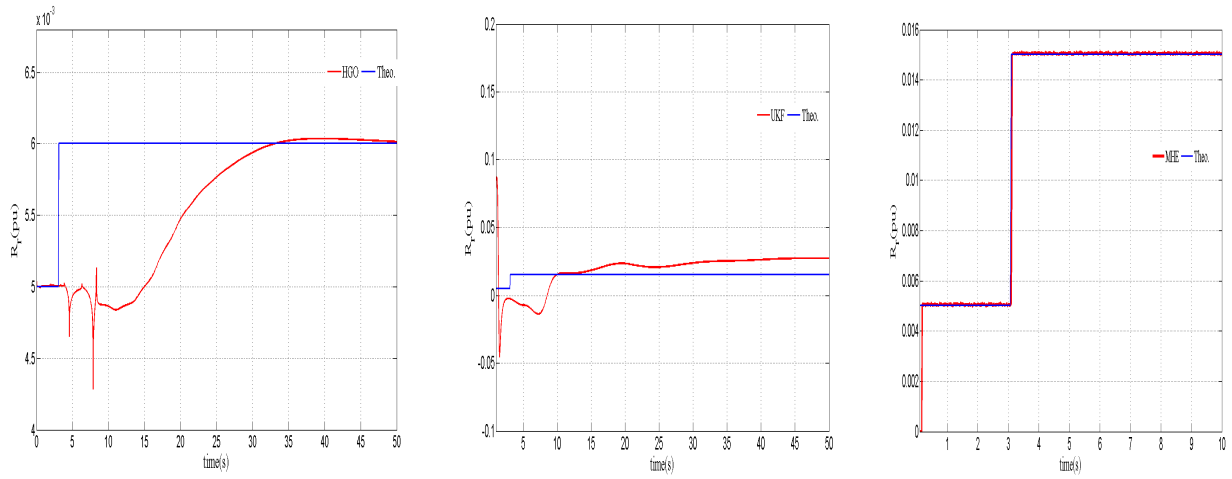
Fig. 3. Parameters estimation in a healthy mode with HGO, UKF and MHE

To verify the robustness, we performed parametric variation on the observer in relation to the identified values. Figures 5 and 6 show the responses obtained when a rotor inductance variation of +50% and -50% is considered for the observer test. The robustness of the observers' scheme with respect to this parameter changes is clearly shown. In Figures 5 and 6, it is clearly shown that a +50% and -50% rotor inductance variation generates a high statistical difference on rotor and stator resistances for the Unscented Kalman Filter. For the High Gain Observer, that variation is much more felt on the rotor resistance on the both figures. Incontestably the Moving Horizon Estimation seems remain insensitive to the parametric variations but it is not so, it is just that the statistical difference generated is weak enough compared to

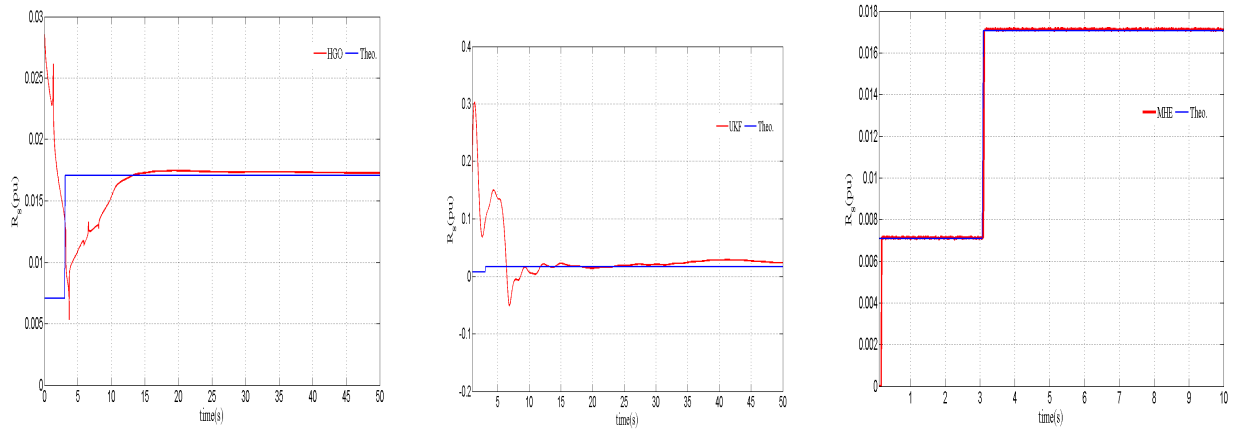
others. From these responses, we can conclude that the rotor inductance changes do not affect the performance of the Moving Horizon Estimation considerably, but in regard to the other observers, the changes disturb their performance a lot as shown in the figures and that the MHE scheme is robust enough under parametric uncertainties.

Table 1. General statistics of the three Observers (Healthy Mode)

	Std(HGO) $\times 10^{-3}$	Std(UKF) $\times 10^{-3}$	Std(MHE) $\times 10^{-3}$
R _s	350	7450	57.75
R _r	7.29	3940	41.38
	Variance(HGO) $\times 10^{-5}$	Variance(UKF) $\times 10^{-5}$	Variance(MHE) $\times 10^{-5}$
R _s	1.26	550	0.033
R _r	0.0053	160	0.017



a) Rotor resistance estimation



b) Stator resistance estimation

Fig 4. Parameters estimation in a faulty mode with HGO, UKF and MHE

Table 2. General statistics of the three Observers (Faulty Mode)

	Std(HGO) $\times 10^{-4}$	Std(UKF) $\times 10^{-4}$	Std(MHE) $\times 10^{-4}$
Rs	25	8208	270
Rr	4.86	278	26
	Variance(HGO) $\times 10^{-5}$	Variance(UKF) $\times 10^{-5}$	Variance(MHE) $\times 10^{-5}$
Rs	0.62	6737	0.74
Rr	0.024	77.47	0.702

Table 3. MSE values of nonlinear observers: HGO, UKF and MHE are compared

	HGO		UKF		MHE	
	Healthy	Faulty	Healthy	Faulty	Healthy	Faulty
Rs	4.73E - 06	8.02E - 06	8.66E - 04	9.65E - 04	1.11E - 07	1.27E - 07
Rr	1.77E - 09	1.79E - 05	9.36E - 05	1.14E - 04	5.71E - 08	7.33E - 08
Φ_{ds}	5.70E - 04	6.31E - 04	9.02E - 05	9.23E - 05	21.0E - 04	11.0E - 04
Φ_{qs}	1.93E - 06	2.10E - 06	1.10E - 16	1.10E - 16	39.0E - 04	27.0E - 04
Φ_{dr}	2.08E - 08	16.00E - 04	6.47E - 06	6.87E - 06	246E - 04	210E - 04
Φ_{qr}	1.73E - 10	4.81E - 06	1.10E - 06	1.10E - 06	67.0E - 04	70.0E - 04

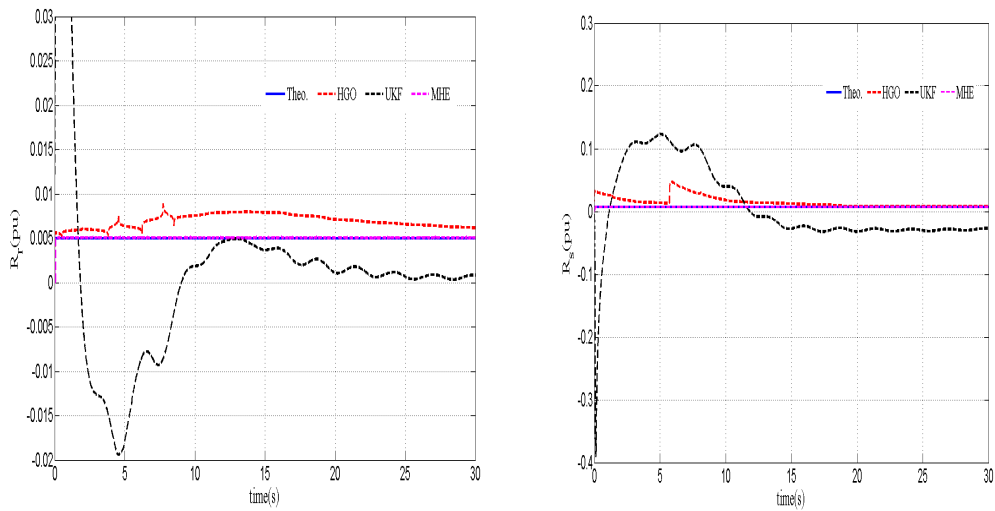


Fig. 5. Robustness test. Rotor inductance variation (+50%)

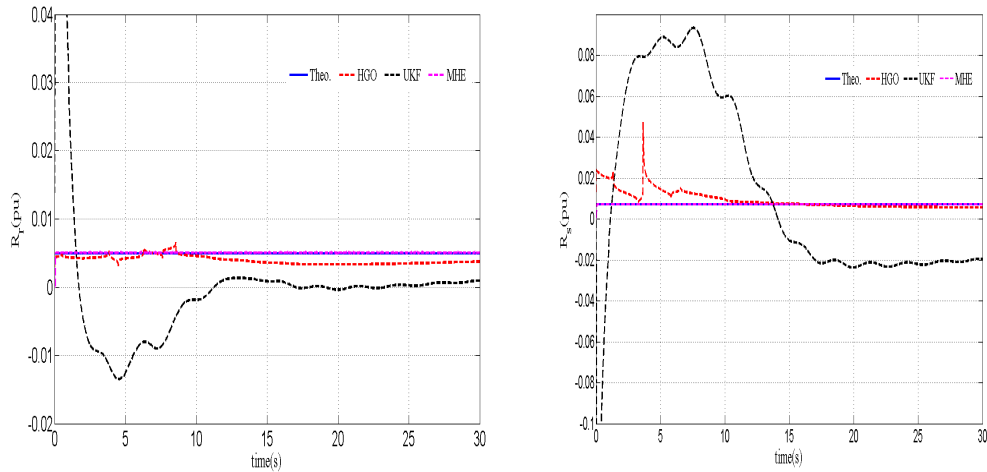


Fig. 6. Robustness test. Rotor inductance variation (-50%)

5. Conclusion

In this paper, a general framework for the doubly fed induction generator has been presented in order to carry out a dynamic estimation of states and parameters of the DFIG. The DFIG parameters are largely influenced by different factors (for instance, temperature, magnetic saturation and eddy current...) that is why it is necessary to develop techniques to estimate the changes of parameters. The proposed techniques are performed with High Gain Observer (HGO), Unscented Kalman Filter (UKF) and Moving Horizon Estimation algorithms using noisy measurements. A comparison of the three estimation techniques has been

made under different aspects notably, computation time and estimation accuracy, in two modes of operation of the DFIG, the healthy mode and the faulty mode. The MHE estimation technique has significantly lower estimation error and converges with fewer samples time than the HGO and the UKF. Whatever the mode of functioning, the simulation results showed that a good standard of performance could be obtained even in the presence of measurement noise.

This is an Open Access article distributed under the terms of the Creative Commons Attribution License



References

- [1] M Tazil, V Kumar, RC Bansal, S Kong, ZY Dong, W Freitas, and HD Mathur. Three-phase doubly fed induction generators: an overview. *IET Electric Power Applications*, 4(2):75-89, 2010.
- [2] Mattia Marinelli, Andrea Morini, Andrea Pitto, Silvestro, and Federico. Modeling of doubly fed induction generator (dfig) equipped wind turbine for dynamic studies. In *Universities Power Engineering Conference, 2008. UPEC 2008. 43rd International*, pages 1-6. IEEE, 2008.
- [3] Shenglong Yu, Kianoush Emami, Tyrone Fernando, Herbert HC Iu, and Kit Po Wong. State estimation of doubly fed induction generator wind turbine in complex power systems. *IEEE Transactions on Power Systems*, 31(6):4935- 4944, 2016.
- [4] R Pena, Clare, JC, Asher, and GM. Doubly fed induction generator using back-to-back pwm converters and its application to variable-speed wind-energy generation. *IEE Proceedings-Electric Power Applications*, 143(3):231-241, 1996.

- [5] Pablo Ledesma, Usaola, and Julio. Doubly fed induction generator model for transient stability analysis. *IEEE transactions on energy conversion*, 20(2):388-397, 2005.
- [6] Kai Rothenhagen and Friedrich W Fuchs. Current sensor fault detection and reconfiguration for a doubly fed induction generator. In *Power Electronics Specialists Conference, 2007. PESC 2007. IEEE*, pages 2732-2738. IEEE, 2007.
- [7] DU Campos-Delgado, DR Espinoza-Trejo, and E Palacios. Fault-tolerant control in variable speed drives: a survey. *IET Electric Power Applications*, 2(2):121-134, 2008.
- [8] Samir Abdelmalek, Sarah Rezazi, Azar, and Ahmad Taher. Sensor faults detection and estimation for a dfig equipped wind turbine. *Energy Procedia*, 139:3-9, 2017.
- [9] K Rothenhagen and FW Fuchs. Model-based fault detection of gain and offset faults in doubly fed induction generators. In *Diagnostics for Electric Machines, Power Electronics and Drives, 2009. SDEMPED 2009. IEEE International Symposium on*, pages 1-6. IEEE, 2009.
- [10] Dihua Li, Xinchun Lin, Sheng Hu, and Yong Kang. An adaptive estimation method for parameters of doubly-fed induction generators (dfig) in wind power controller. In *Power and Energy Engineering Conference (APPEEC), 2010 Asia-Pacific*, pages 1-4. IEEE, 2010.
- [11] Simon J Julier, Uhlmann, and Jeffrey K. New extension of the Kalman filter to nonlinear systems. In *Signal processing, sensor fusion, and target recognition VI*, volume 3068, pages 182-194. International Society for Optics and Photonics, 1997.
- [12] Eric A Wan, Van Der Merwe, and Rudolph. The unscented Kalman filter for nonlinear estimation. In *Adaptive Systems for Signal Processing, Communications, and Control Symposium 2000. AS-SPCC. The IEEE 2000*, pages 153-158. Ieee, 2000.
- [13] Abdelhak Dida, Attous, and Djilani Ben. Doubly-fed induction generator drive based wecs using fuzzy logic controller. *Frontiers in Energy*, 9(3):272-281, 2015.
- [14] Xueping Pan, Ping Ju, Feng Wu, and Yuqing Jin. Hierarchical parameter estimation of dfig and drive train system in a wind turbine generator. *Frontiers of Mechanical Engineering*, 12(3):367-376, 2017.
- [15] Siegfried Heier. Wind energy conversion systems. *Grid Integration of Wind Energy: Onshore and Offshore Conversion Systems*, pages 31-117, 2014.
- [16] W Leonhard. Controlled ac drives, a successful transition from ideas to industrial practice. *Control Engineering Practice*, 4(7):897-908, 1996.
- [17] Lihui Yang, Zhao Xu, Jacob Østergaard, Zhao Yang Dong, Kit Po Wong, and Xikui Ma. Oscillatory stability and eigenvalue sensitivity analysis of a dfig wind turbine system. *IEEE Transactions on Energy Conversion*, 26(1):328-339, 2011.
- [18] Alexandre Teplaira Boum and S.A. Talla. High gain observer and moving horizon estimation for parameters estimation and fault detection of an induction machine: A comparative study. *Journal of Control and Instrumentation*, 8:15-26, 08 2017
- [19] Henk Nijmeijer and Thor I Fossen. *New directions in nonlinear observer design*, volume 244. Springer, 1999.
- [20] Guy Bornard and H Hammouri. A high gain observer for a class of uniformly observable systems. In *Decision and Control, 1991. Proceedings of the 30th IEEE Conference on*, pages 1494-1496. IEEE, 1991.
- [21] Matthew Rhudy and Yu Gu. Understanding nonlinear Kalman filters, part ii: An implementation guide. *Interactive Robotics Letters*, 2013.
- [22] Jean-Pierre Corriou. *Process control*. Springer, 2004.
- [23] Michalska, Hannah, Mayne, and David Q. Moving horizon observers and observer-based control. *IEEE Transactions on Automatic Control*, 40(6):995-1006, 1995.
- [24] Rao, Christopher V, Rawlings, James B, and Jay H Lee. Constrained linear state estimation-a moving horizon approach. *Automatica*, 37(10):1619-1628, 2001.
- [25] Douglas G Robertson, Jay H Lee, and James B Rawlings. A moving horizon-based approach for least-squares estimation. *AIChE Journal*, 42(8):2209-2224, 1996.
- [26] Slotine, J-JE, Hedrick, JK, and EA Misawa. On sliding observers for nonlinear systems. *Journal of Dynamic Systems, Measurement, and Control*, 109(3):245-252, 1987.
- [27] J.P. Gauthier, H. Hammouri, and S. Othman. A simple observer for nonlinear systems applications to bioreactors. *IEEE Transactions on automatic control*, 37(6):1875, 1992.

Appendix

Table 4. Parameters of the DFIG

Parameters	Values
Rated active power (Ps)/(MW)	1.5
Rated voltage (line to line) (Vs)/(V)	575
Rated DC-link voltage (Vdc)/(V)	1200
Number of poles	4
frequency(f)/(Hz)	60
Stator resistance (Rs)/(pu)	0.00707
Rotor resistance (Rr)/(pu)	0.005
Stator leakage inductance (Ls)/(pu)	0.171
Rotor leakage inductance (Lr)/(pu)	0.156
Magnetizing inductance (Lm)/(pu)	2.9
DC-link capacitance (C)/(F)	0.04

Table 5. Parameters of the wind turbine

Parameters	Values
Rated wind speed (v_w)/(m.s-1)	12
Number of blade	3
Radius of blade (R)/m	35.25
Gearbox gain (G)	91
Moment of inertia (J_{eq})/(kg.m2)	1000
Viscosity factor (f_{eq})/(N.m.s.rad-1)	0.0024

Table 6. MHE parameters

Parameters	Values
Weight matrix G	eye(6)
Covariance matrix P_0	3eye(6)
Covariance matrix Q	0.5eye(6)
Covariance matrix R	eye(5)
Length horizon H	10

Initial guess	[0; 0.5; 0.5; 1; 0.02; 0.02]
---------------	------------------------------

Table 7. UKF parameters

Parameters	Values
Covariance matrix P_0	eye(6)
Covariance matrix Q	$10^{-2} \text{diag}([111110-410-4])$
Covariance matrix R	$10^{-2} \text{diag}([11111])$
Initial guess	[0; 0.5; 0.5; 1; 0.02; 0.02]

Table 8. Running time of the three observers for the DFIG (seconds)

	HGO	UKF	MHE
Healthy mode	1.200	1.190	152.978
Faulty mode	1.901	1.666	154.234